Acta of Bioengineering and Biomechanics
Vol. 16, No. 3, 2014

Original paper
DOI: 10.5277/abb140306

Comparison of constitutive models of arterial layers with distributed collagen fibre orientations

PAVEL SKACEL*, JIRI BURSA

Institute of Solid Mechanics, Mechatronics and Biomechanics, Brno University of Technology, Brno, Czech Republic.

Several constitutive models have been proposed for description of mechanical behaviour of soft tissues containing collagen fibres. The model with aligned fibres is modified in this paper to take the dispersion of fibre orientations into account through angular integration and it is compared with the model that is defined through generalized structure tensor. The paper is focused on the effect of fibre dispersion on the resulting stress-strain behaviour predicted by both models analyzed. Analytical calculations are used for the comparison of the mechanical behaviour under a specific biaxial tension mode. The two models have been implemented into commercial finite element code ANSYS via user subroutines and used for numerical simulation resulting in a non-homogeneous stress field. The effects of the fibre dispersion predicted by both models being compared differ significantly, e.g., the resulting stress difference between both models is lower than 10% only in the case of extremely small dispersion of collagen fibres orientation ($\kappa < (0.01 \text{ to } 0.03)$). These results are consistent with those of other related literature. The applicability of the model defined through the generalized structure tensor is discussed.

Key words: *arterial wall mechanics, collagen fibre orientation, constitutive modelling, fibre distribution, hyperfit software*

1. Introduction

Several constitutive models have been proposed for description of soft tissue mechanics. Most of soft tissues exhibit a strongly progressive character of their stress-strain relationships that is usually attributed to the straightening of the (collagen) fibres and often modelled by exponential functions. Several phenomenological exponential models have been proposed, analyzed and used for description of a variety of soft tissues (e.g. [1]–[3] for isotropic models; [4]–[9] for anisotropic forms).

From the micro-structural point of view the fibre constituents of most soft tissues are significantly dispersed in their orientations. According to polarized light microscopy investigations of arterial layers ([10]–[12]) the collagen fibres (as well as smooth muscle cells) are aligned rather coherently in media layers whereas the collagen orientation in the adventitia layer is significantly dispersed. The angular distribution of fibres (obtained by small angle light scattering method) for aortic valve and bovine pericardium was presented in [13]. Recently, the quantitative data related to the distribution of collagen fibres of thoracic and abdominal aortas (and common iliac arteries) [14] and of abdominal aortic aneurysms [15] have been published.

A phenomenological model with some structural parameters has been proposed by Holzapfel et al. [16] specifically for arterial layers. This model distinguishes the contributions of individual structural components (non-collagenous matrix and collagen fibres) and assumes two symmetrical families of perfectly aligned (i.e., non-dispersed) collagen fibres. Gasser et al. [17] proposed a similar model for arterial layers accounting also for the dispersion of fibre orientations. Several other authors ([18], [19], [13], [20], [21]) presented their proposals of micro-structural constitutive models for various soft tissues accounting

* Corresponding author: Pavel Skacel, Institute of Solid Mechanics, Mechatronics and Biomechanics, Brno University of Technology, Technicka 2896/2, 616 69 Brno, Czech Republic. Tel:+420 5 4114 2868, Fax: 420 5 4114 2876, e-mail: skacel@fme.vutbr.cz, bursa@fme.vutbr.cz

Received: August 15th, 2013
Accepted for publication: February 7th, 2014

for the distribution of the fibre orientations and/or the distribution of the fibre crimps, usually based on the work of Lanir [22].

In this paper, two specific anisotropic models originally proposed for description of passive stress-strain behaviour of arteries (but frequently used also for other fibrous soft tissues, e.g.. cornea and skin [23]–[25]) are analyzed. First, the model with perfectly aligned (collagen) fibres proposed by Holzapfel et al. [16] and modified recently in [26] (using the approach of Lanir [22]) to account for the distribution of fibre orientations, and second, the frequently applied model proposed by Gasser et al. [17] accounting for this dispersion in a simplified manner. The effect of fibre dispersion on the resulting stress-strain behaviour of both models is investigated and compared in this paper. A similar comparative analysis [26] of these models is extended here for two families of fibres and aimed at parameter values and range of stretches typical of arterial layers.

2. Constitutive models

The model with perfectly aligned collagen fibres proposed by Holzapfel et al. [16] (called HGO model in this text) is introduced in section 2.1. Using the approach of Lanir [22] the HGO model can be modified to take the angular dispersion of fibres into account; the resulting model (called AI model ~ Angular Integration Model, consistently with [26]) is presented in Section 2.2. An equivalent model implementing angular dispersion of fibres is introduced in Section 2.3; it was previously proposed by Gasser et al. [17] and is called GST model in this text (Generalized Structure Tensor model, consistently with [26]).

The following incompressible formulation is shared by all the hyperelastic models analyzed

$$\Psi(\mathbf{C}) = \Psi_g(\mathbf{C}) + \sum_{i=1,2} \Psi_{fi}(\mathbf{C}), \tag{1}$$

$$\Psi_g(\mathbf{C}) = \frac{c}{2}(I_1 - 3), \tag{2}$$

where Ψ is the elastic strain energy density; Ψ_g and Ψ_{fi} are its contributions related to non-collagenous ground matrix and to two (i = 1, 2) families of (collagen) fibres, respectively; $c > 0$ is a stress-like material parameter related to ground matrix; I_1 is the first invariant of the right Cauchy–Green deformation tensor $\mathbf{C} = \mathbf{F}^T\mathbf{F}$; $\mathbf{F}$ is the deformation gradient.

Although the structurally-based approaches for Ψ_g (reflecting the fibrous nature of elastin constituent) have already been proposed and used by some researchers (e.g., [22], [27]), the neo-Hookean model (2) is considered for all the constitutive models compared (adopted from [16], [17] and consistent with [26]) although not capable to predict eventual buckling of the non-collagenous (elastin) fibres. Moreover, this approach allows us to reduce the number of (generally unknown) material parameters effectively and to focus on the main objective of this paper, namely the effect of collagen fibre dispersion and different ways of its description by the models compared.

2.1. HGO model

HGO model assumes the following relation for the strain energy density of fibres

$$\Psi_{fi}^{\mathrm{HGO}}(\mathbf{C}, \mathbf{A_{0i}}) = \frac{k_1}{2k_2}\{\exp[k_2(I_{4i} - 1)^2] - 1\}, \tag{3}$$

$$I_{4i} = \mathbf{A_{0i}} : \mathbf{C}, \quad \mathbf{A_{0i}} = \mathbf{a_{0i}} \otimes \mathbf{a_{0i}},$$

$$\mathbf{a_{0i}} = \begin{bmatrix} \sin\Theta_i \cos\Phi_i \\ \sin\Theta_i \sin\Phi_i \\ \cos\Theta_i \end{bmatrix}, \tag{4}$$

where $k_1 > 0$ and $k_2 > 0$ are stress-like and dimensionless material parameters, respectively referenced to (collagen) fibre properties; I_{4i} is a (pseudo)invariant of $\mathbf{C}$ and $\mathbf{A_{0i}}$ associated with the contribution of the i-th (collagen) fibre family and representing directly the squared stretch of this fibre family. It is supposed that collagen fibres are inactive in compression, therefore relation (3) is used only if $I_{4i} \geq 1$. The unit vectors $\mathbf{a_{0i}}$ define the directions of two (i = 1, 2) fibre families in the reference configuration and are specified by angles Θ_i, Φ_i related to spherical polar coordinates (see Fig. 1). The model assumes two perfectly aligned fibre families that are mechanically equivalent and

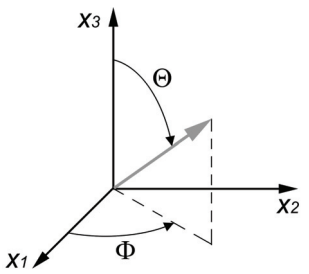

Fig. 1. Characterization of angles Θ, Φ used for definition of fibre orientation

embedded in the ground matrix. The following material parameters are required for HGO model: c, k_1, k_2, $\mathbf{a_{01}}$, $\mathbf{a_{02}}$.

2.2. AI model

In the case of AI model the effect of distributed fibre orientation is implemented by summing the contributions of fibres in all directions. The approach based on the superposition principle was originally applied by Lanir [22] and followed by many others ([19], [18], [13], [20], [21]). In this sense the strain energy function of the HGO model applied for distributed fibre orientations may take the form

$$\Psi_{fi}^{\mathrm{AI}}(\mathbf{C},\mathbf{a_{0i}^m}) = \frac{1}{4\pi}\int_{\omega} \rho_{i(\Theta,\Phi)} \Psi_{fi}^{\mathrm{HGO}}(\mathbf{C},\mathbf{A_{0i(\Theta,\Phi)}})\, d\varpi\,, \quad (5)$$

$$\mathbf{A_{0i}} = \mathbf{a_{0i(\Theta,\Phi)}} \otimes \mathbf{a_{0i(\Theta,\Phi)}}\,, \quad \mathbf{a_{0i(\Theta,\Phi)}} = \begin{bmatrix} \sin\Theta\cos\Phi \\ \sin\Theta\sin\Phi \\ \cos\Theta \end{bmatrix}, \quad (6)$$

where Θ and Φ are Eulerian angles according to Fig. 1, ϖ is the unit sphere, $d\varpi = \sin(\Theta)\, d\Theta\, d\Phi$ and ρ_i is the probabilistic distribution function (PDF) of fibre orientation (within the i-th fibre family and normalized such that $1/(4\pi)\int_{\omega} \rho_{i(\Theta,\Phi)}\, d\varpi = 1$). Notice that the structure tensor $\mathbf{A_{0i}}$ is now a function of orientation angles Θ, Φ. To be consistent with GST model (Section 2.3) the fibres within the given i-th family are assumed to be distributed with rotational symmetry about a mean referential (preferred) direction $\mathbf{a_{0i}^m} = [\sin\Theta_i^m \cos\Phi_i^m,\ \sin\Theta_i^m \sin\Phi_i^m,\ \cos\Theta_i^m]^{\mathrm{T}}$. Θ_i^m and Φ_i^m are angular parameters defining the mean direction of fibres within a given (i-th) family in the referential (undeformed) configuration.

Transversely isotropic and π-periodic von-Mises PDF was adopted from [17] that takes the form

$$\rho_{i(\Theta,\Phi)} = 4\sqrt{\frac{b}{2\pi}}\, \frac{\exp[b(\cos(2\chi_{i(\Theta,\Phi)})+1)]}{\mathrm{erfi}(\sqrt{2b})} \quad (7)$$

where b is the concentration parameter, erfi(x) is the imaginary error function, and χ_i is the angle between vectors $\mathbf{a_{0i}}$ and $\mathbf{a_{0i}^m}$ (i.e., an inclination angle of orientation given by the vector $\mathbf{a_{0i}}$ from the mean direction of fibres given by $\mathbf{a_{0i}^m}$ for the i-th fibre family).

The model contains an equivalent set of material parameters to the HGO model (c, k_1, k_2, $\mathbf{a_{01}^m}$, $\mathbf{a_{02}^m}$) extended by the concentration parameter b. For a specific case of perfectly aligned fibres (no fibre dispersion, $b = \infty$) the model coincides with the HGO model (3). For another specific case of fully dispersed fibres (uniform distribution $\rho = 1$, $b = 0$) the model becomes isotropic and independent of the mean orientation $\mathbf{a_{0i}^m}$. The application of the AI model requires integration over spherical polar coordinates Θ, Φ.

2.3. GST model

The concept of the GST model is based on the definition of a generalized structure tensor $\mathbf{H}$ [17] that is derived from (classical) structure tensor $\mathbf{M}$ distributed through PDF ρ (in an effort to represent the effect of distributed fibres in a continuum sense)

$$\mathbf{H} = \frac{1}{4\pi}\int_{\omega} \rho_{(\Theta,\Phi)} \mathbf{M}_{(\Theta,\Phi)}\, d\varpi\,. \quad (8)$$

As shown in [17], for any transversely isotropic PDF the resulting generalized structure tensor can be given in a compact form $\mathbf{H} = \kappa\mathbf{I} + (1-3\kappa)\mathbf{A_0}$ (where $\mathbf{I}$ is the identity tensor and $\mathbf{A_0} = \mathbf{a_0^m} \otimes \mathbf{a_0^m}$ is a structure tensor defined using unit vector $\mathbf{a_0^m}$ specifying the mean orientation of fibres ~ axis of distribution function ρ). The distribution function ρ is then fully characterized only by a single parameter κ, called dispersion parameter

$$\kappa = \frac{1}{4}\int_0^{\pi} \rho_{(\chi)} \sin^3\chi d\chi \quad (9)$$

where χ is the inclination angle with respect to ρ axis.

Gasser et al. [17] replaced the (classical) structure tensor $\mathbf{A_0}$ in the constitutive form (3) of HGO model by the generalized structure tensor $\mathbf{H}$ and proposed a new constitutive model

$$\Psi_{fi}^{\mathbf{GST}}(\mathbf{C},\mathbf{H_i}) = \frac{k_1}{2k_2}\{\exp[k_2(I_i^*-1)^2]-1\}\,, \quad (10)$$

$$I_i^* = \kappa I_1 + (1-3\kappa) I_{4i}\,, \quad I_{4i} = \mathbf{A_{0i}} : \mathbf{C}\,,$$

$$\mathbf{A_{0i}} = \mathbf{a_{0i}^m} \otimes \mathbf{a_{0i}^m}\,, \quad (11)$$

where I_i^* is a quantity related to $\mathbf{C}$, combining its I_1 and I_{4i} (pseudo)invariants and representing a deformation measure of the i-th fibre family with mean orientation $\mathbf{a_{0i}^m}$. Similarly to HGO model the aniso-

tropic part of I_i^* is considered only if $I_{4i} \geq 1$ (~ if the strain in the mean fibre direction $\mathbf{a}_{0i}^{m}$ is positive).

The GST model has the same set of material parameters (c, k_1, k_2, $\mathbf{a}_{01}^{m}$, $\mathbf{a}_{02}^{m}$, κ) as AI model except for the fact that the dispersion parameter κ is used instead of the concentration parameter b. Nevertheless, these parameters are in a direct mutual relation through equation (9) (see graph in Fig. 2) and one value of $\kappa \in \langle 1/3, 0\rangle$ always corresponds to each $b \in \langle 0, \infty\rangle$, as already shown in [17]. For a specific case of perfectly aligned fibres (no fibre dispersion, $\kappa = 0$, $I_i^* = I_{4i}$) the model coincides with the HGO model (3). For another specific case of fully dispersed fibres (uniform distribution, $\kappa = 1/3$, $I_i^* = I_1/3$) the model becomes purely isotropic and independent of the mean orientation $\mathbf{a}_{0i}^{m}$. The compact form of the model is beneficial for its numerical application. Note that very little formal change is sufficient to reach GST model definition (10) from HGO model definition (3) – just to replace I_4 by I^*. This often leads to a statement that such a "small modification of the fourth invariant is able to represent the dispersion of collagen fibre orientation" (cited from [28]). The validity of this statement is analyzed in the following sections through a direct comparison between the GST model and the AI model.

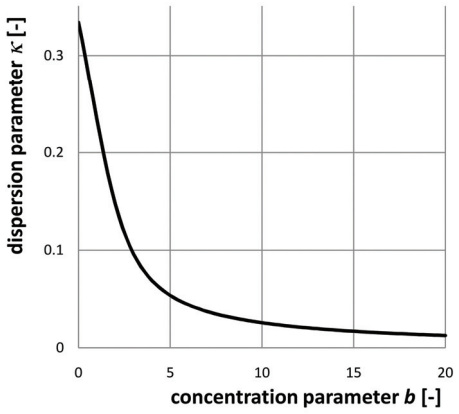

Fig. 2. Relation between the dispersion parameter κ and the concentration parameter b

3. Methods and results

The analysis in this paper provides analytical calculation and results with respect to conditions typical of arterial layers with maximum stretch λ up to 1.5. The effect of a specific constitutive model and the effect of material progressivity parameter (k_2) is investigated. The paper provides also an example of finite element (FE) calculation based on the user subroutine implementation into a commercial FE code (ANSYS) that proves the FE applicability of the full-integration models.

3.1. Analytical calculations

Based on the theory of incompressible hyperelastic solids, the constitutive models introduced above result in the Cauchy stress

$$\boldsymbol{\sigma} = -p\mathbf{I} + 2\frac{\partial \Psi}{\partial I_1}\mathbf{B} + 2\frac{\partial \Psi}{\partial I_4}\mathbf{A} \tag{12}$$

where p is the Lagrange multiplier, $\mathbf{I}$ is the identity tensor, $\mathbf{B} = \mathbf{F}\mathbf{F}^T$ is left Cauchy–Green deformation tensor and $\mathbf{A} = \mathbf{F}\mathbf{a}_0 \otimes \mathbf{F}\mathbf{a}_0$. When applied to the AI model, the stress calculation can be manipulated in the following form (that has to be solved numerically)

$$\boldsymbol{\sigma}^{\mathrm{AI}} = -p\mathbf{I} + c\mathbf{B} + \frac{k_1}{2\pi}\int_0^{2\pi}\int_0^{\pi}(\rho_1+\rho_2)(I_4-1)\exp[k_2(I_4-1)^2]\mathbf{A}\sin\Theta d\Theta d\Phi. \tag{13}$$

When applied to the GST model, the calculation of stress $\boldsymbol{\sigma}^{\mathrm{GST}}$ (defined by equations (10)–(12)) is relatively straightforward using the following response functions

$$\frac{\partial \Psi}{\partial I_1} = \frac{c}{2} + \sum_{i=1}^{2} k_1\kappa E_i \exp(k_2 E_i^2),$$
$$\frac{\partial \Psi}{\partial I_{4i}} = k_1(1-3\kappa)E_i \exp(k_2 E_i^2), \tag{14}$$

with the substitution parameter E_i representing a Green–Lagrange strain-like quantity and characterizing the average stretch within the i-th family of collagen fibres

$$E_i = \mathbf{H}:\mathbf{C} - 1 = \kappa(I_1 - 3) + (1-3\kappa)(I_{4i} - 1). \tag{15}$$

A specific deformation (see Fig. 3) defined by $\mathbf{F} = \mathbf{diag}[\lambda, 1, \lambda^{-1}]$ is considered with parameter λ representing the stretch ratio in direction x_1. This deformation mode is equivalent to deformation of the cylindrical vessel wall with the fixed axial length and loaded by inner pressure. Two fibre families with mean orientations in x_1–x_2 plane are considered

$$\Theta_1^m = \Theta_2^m = \frac{\pi}{2}; \quad \Phi_1^m = \varphi; \quad \Phi_2^m = -\varphi. \tag{16}$$

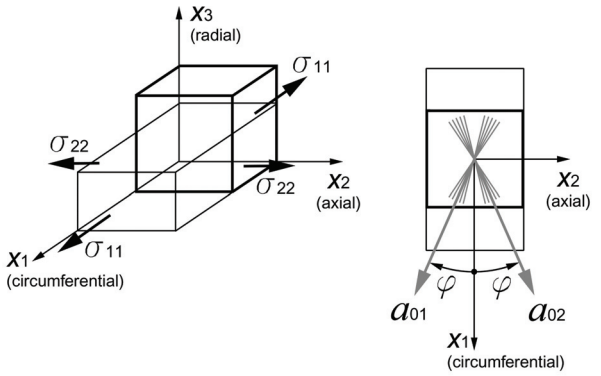

Fig. 3. Scheme of deformation mode considered for analytical calculations

Due to the symmetry no shear accompanies the deformation, and therefore the biaxial stress state $\boldsymbol{\sigma} = \mathbf{diag}[\sigma_{11}, \sigma_{22}, 0]$ can be considered. The σ_{11} component of stress (that is expected to be dominant and corresponds to tangential stress in the virtual cylindrical vessel) is used for further comparison between the specific constitutive models. For simplicity, σ_{22} stress is omitted from the comparison since this component (corresponding to axial stress in the virtual cylindrical vessel) is expected to be minor in comparison with σ_{11}. The Lagrange multiplier p can be eliminated using the boundary condition ($\sigma_{33} = 0$) and then σ_{11} depends on five material parameters: c, k_1, k_2, φ, b (or κ). The constitutive models compared differ only in fibre-related contributions (which usually dominate at higher stretches), therefore the effect of matrix on stresses can be excluded by $c = 0$. The resulting (fibre) stresses are then proportional to k_1 parameter, therefore the normalized stress σ^* (depending only on three material parameters k_2, φ, b or κ) is introduced as follows and used for the comparison presented.

$$\sigma^* = \sigma_{11} / k_1 . \tag{17}$$

A variety of analytical calculations have been performed for different combinations of the material parameters.

For a specific case of fully-dispersed (i.e., uniformly distributed) fibres ($b = 0$), the stress-stretch relations should be independent of the mean orientations of fibre families. This fundamental assumption is not fully met by GST model ($\mathbf{a}_{0i}^{m}$ vector influences tension/compression status of the whole fibre family) and therefore the application of GST model to uniform fibre distribution is a priori questionable. In spite of this fact, the associated stress-stretch responses were calculated and compared in Fig. 4. It can be clearly seen that AI model exhibits much stiffer behaviour than GST model. In addition to the great quantitative differences, there is also a significant qualitative difference – AI model exhibits non-zero initial stiffness while it is zero for GST model. The response of HGO model (with perfectly aligned fibres in three different directions) is included in Fig. 4 for evaluation of the dispersion effect on the stress-stretch response. The response of AI model is similar to the response of a model with perfectly aligned fibres oriented in $\varphi = 45°$.

For non-uniformly dispersed fibres ($b > 0$), the stress-stretch response depends on the mean orientation angle φ – the resulting responses of the models are compared in Fig. 5. It is evident that for highly organized fibres ($b = 20$) both the compared models

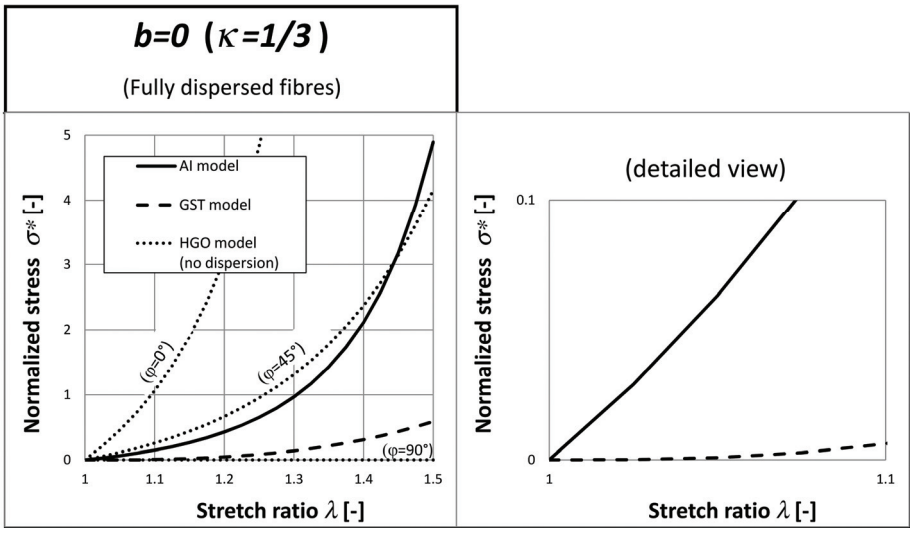

Fig. 4. Stress-stretch responses of constitutive models for fully dispersed fibres (and for fixed $k_2 = 1$). Note that fibre direction (φ) dependent response of HGO model is included (dotted lines) even though it is unable to describe the fibre dispersion. Comparison of initial stiffnesses is shown in detailed view on the right

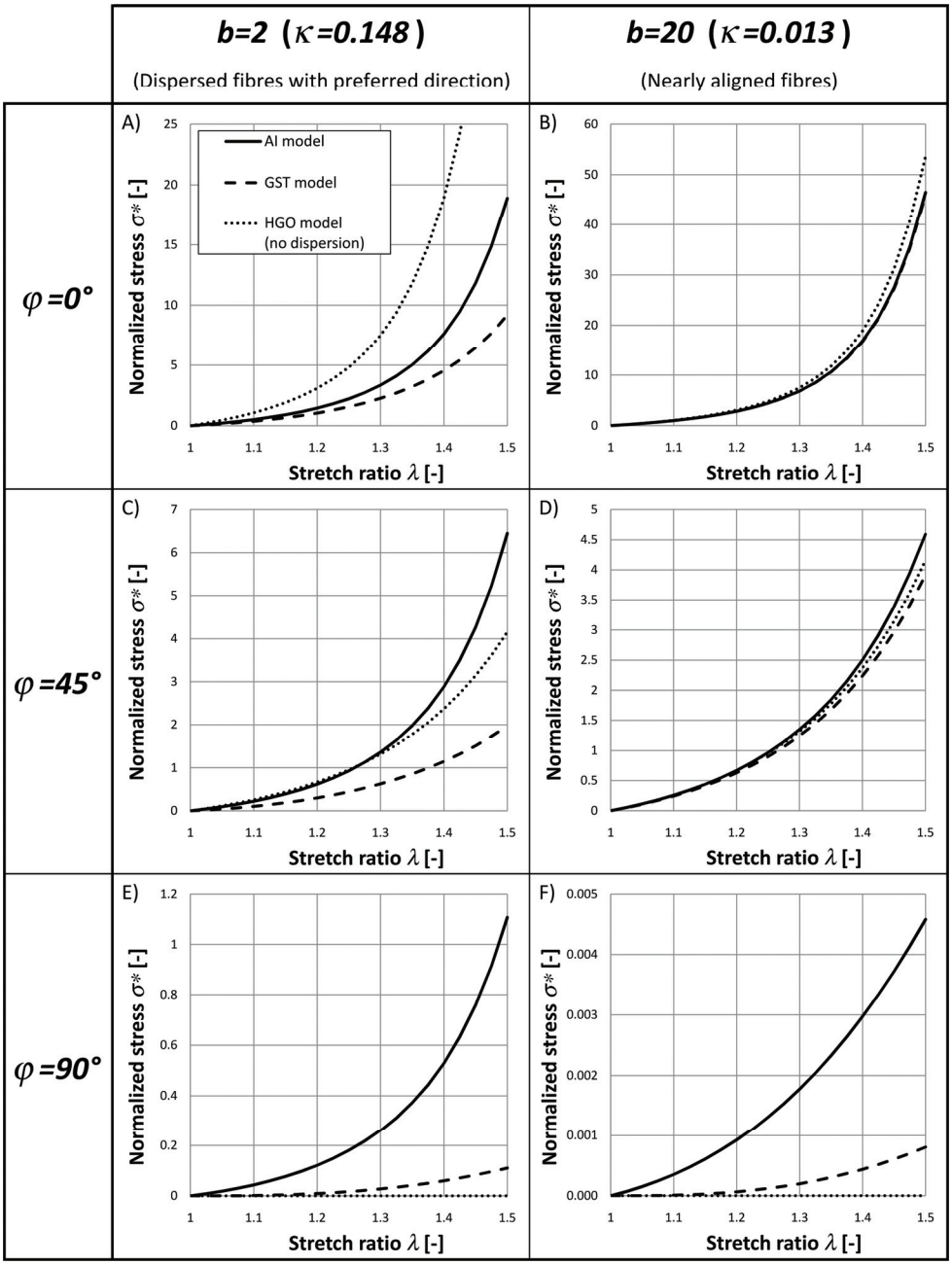

Fig. 5. Stress-stretch responses of constitutive models for various amounts of dispersion and for various orientation angles φ of fibres (fixed $k_2 = 1$)

coincide with HGO model (see Fig. 5B, D, F) as expected. For the case of dispersed fibres (b = 2) the responses of both models compared exhibit significant differences from HGO model and also from each other (see Fig. 5A, C, E). The results confirm an intuitive expectation that for orientation of fibres transversal to the load (φ = 90°), the fibre dispersion stiffens the material and softens it for their longitudinal orientation (φ = 0°). The results also indicate that the response of GST model tends always to be softer than the response predicted by AI model.

$\Delta\sigma$ is introduced as a relative stress difference between the models analyzed

$$\Delta\sigma = \frac{\sigma_{11}^{\mathrm{GST}} - \sigma_{11}^{\mathrm{AI}}}{\sigma_{11}^{\mathrm{AI}}} = \frac{\sigma^{*\mathrm{GST}} - \sigma^{*\mathrm{AI}}}{\sigma^{*\mathrm{AI}}} \tag{18}$$

where superscripts GST and AI denote the stresses (and normalized stresses) related to GST and AI models, respectively. Figure 6 shows the summary of the stress difference $\Delta\sigma$ as a function of λ, κ (or b) and φ (for fixed k_2 = 1). The effect of parameter k_2 is presented separately in Fig. 7 and shows that even higher

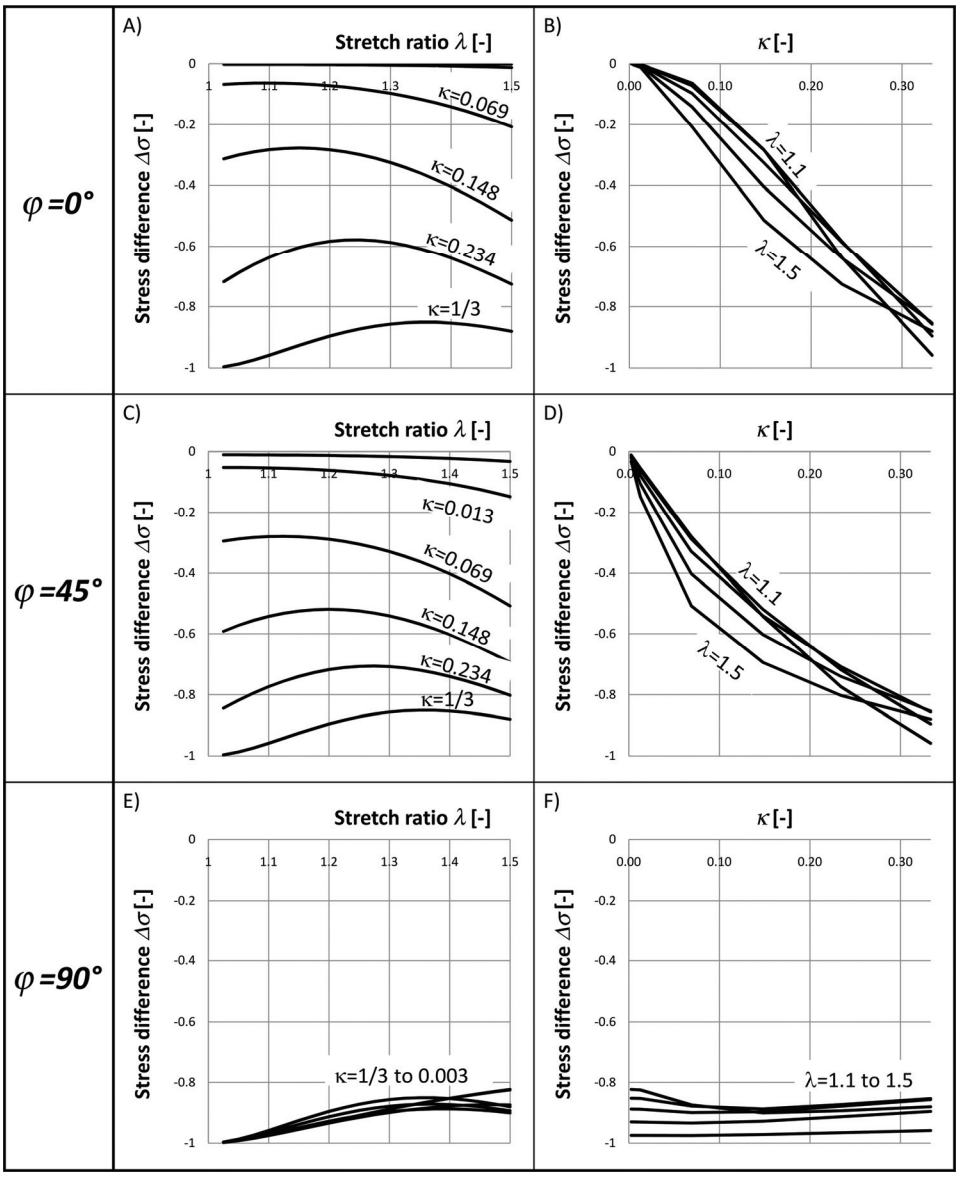

Fig. 6. Stress difference $\Delta\sigma$ between GST and AI models as a function of stretch ratio λ (left column) and/or as a function of dispersion parameter κ (right column), (fixed $k_2 = 1$)

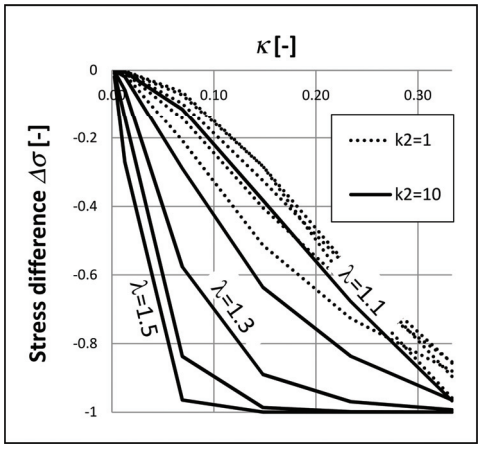

Fig. 7. The effect of k_2 parameter on stress difference $\Delta\sigma$ as a function of dispersion parameter κ, (fixed $\varphi = 0°$)

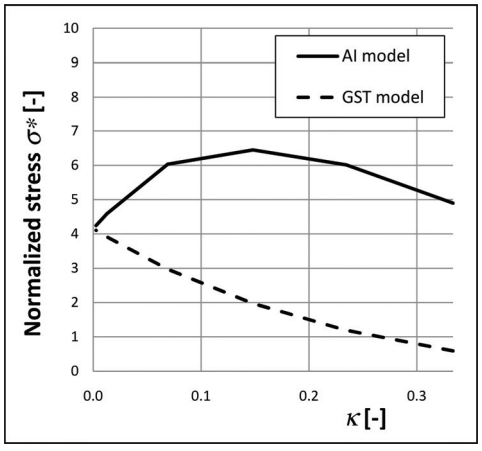

Fig. 8. The effect of dispersion parameter κ on stress σ^* predicted by different constitutive models (fixed $\varphi = 45°$, $k_2 = 1$)

stress difference $\Delta\sigma$ is associated with the increased parameter k_2. Moreover, while the relative difference $\Delta\sigma$ is nearly independent of the stretch ratio (see Fig, 6B, D, F), this dependence is becoming more pronounced with increasing k_2 value.

Figure 8 compares directly the effect of dispersion on the stress predicted by both of the models analyzed. This figure clearly demonstrates that qualitatively different predictions (with respect to fibre angular dispersion) can be provided by the constitutive models analyzed.

3.2. Finite element calculations

Finite element (FE) simulation of uniaxial tensile test performed with iliac adventitial strips (see Fig. 9) was previously used in [17] to demonstrate the influence of angular dispersion of fibres on the resulting mechanical responses of the GST model. The same analysis is used in this paper with equivalent aims – to demonstrate the differences related to AI model, to prove its numerical applicability and to verify the above analytical results indicating a significant discrepancy between the predictions of the two models compared. Geometry parameters (referential length l = 10.0 mm, width w = 3.0 mm, thickness t = 0.5 mm), material parameters (c = 7.64 kPa, k_1 = 996.6 kPa, k_2 = 524.6, φ = 49.98°, κ = 0.226 or b = 1.084), FE mesh density (4 × 20 × 40 = 3200 elements) and loading (tensile load T = 0 to 1 N) were adopted from [17]. All the constitutive models analyzed were implemented as user subroutines into commercial FE code ANSYS 12.0.

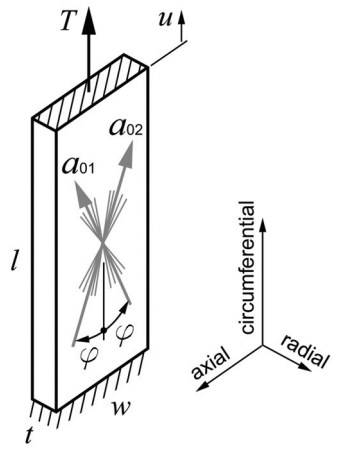

Fig. 9. Scheme of uniaxial tensile test on an adventitial strip used for FE numerical simulation

AI model is more time-consuming for FE calculations (due to the numerical integrations related to equation (5)) – time of FE iteration was approx. 5 times longer than for GST model (however, this ratio cannot be generalized). Lebedev quadrature [29] was used for numerical integration over the sphere domain ω. The accuracy of the numerical integration used was proved to be within 1% of stress error. Details regarding the efficient numerical integration methods suitable for the specific AI model are currently being published in the separate analysis [30]. The results of FE simulations related to different constitutive models are depicted in Fig. 10 and Fig. 11. The same output quantities as used in [17] and the same contour colours were intentionally chosen for Fig. 10 comparing both independent FE solutions (FEAP versus ANSYS). The results show that the strong anisotropy caused by perfectly aligned fibres (HGO model) results in a non-realistic deformation with significant transversal expansion in the radial direction of the wall, while both implementations of fibre angular dispersion (HGO and AI models) lead to a qualitatively acceptable deformation response of the specimen. Nevertheless, the results of GST model are strongly different from the results of AI model. The difference visible in Fig. 10 is attributed to the much stiffer and more homogenous response of AI model, as depicted in Fig. 11, which compares the influence of fibre dispersion on the global force-displacement (T–u) response predicted by GST and AI models.

To demonstrate the FE applicability of AI model under large deformation, its material parameters were adjusted (k_1 = 24.7 kPa, k_2 = 13.7) so that the AI model exhibits practically identical uniaxial stress-strain behaviour as GST model (see Fig. 12). Structural parameters φ and b (and matrix-related parameter c) were considered as fixed. A specific purpose software HYPERFIT (commercially available at www.hyperfit.wz.cz) was used to fit the *AI model* on the response of the GST model. This approach simulates the (practical) situation when both constitutive models are fitted to the same experimental data. Figure 12 shows that AI model is able to approximate well the macroscopic stress-strain response of GST model, when needed. The resulting deformation and stress distribution of the FE calculation can be seen in Fig. 13 that documents the more homogenous stress field of AI model (compared to GST model) even under large deformation with macroscopically equivalent response.

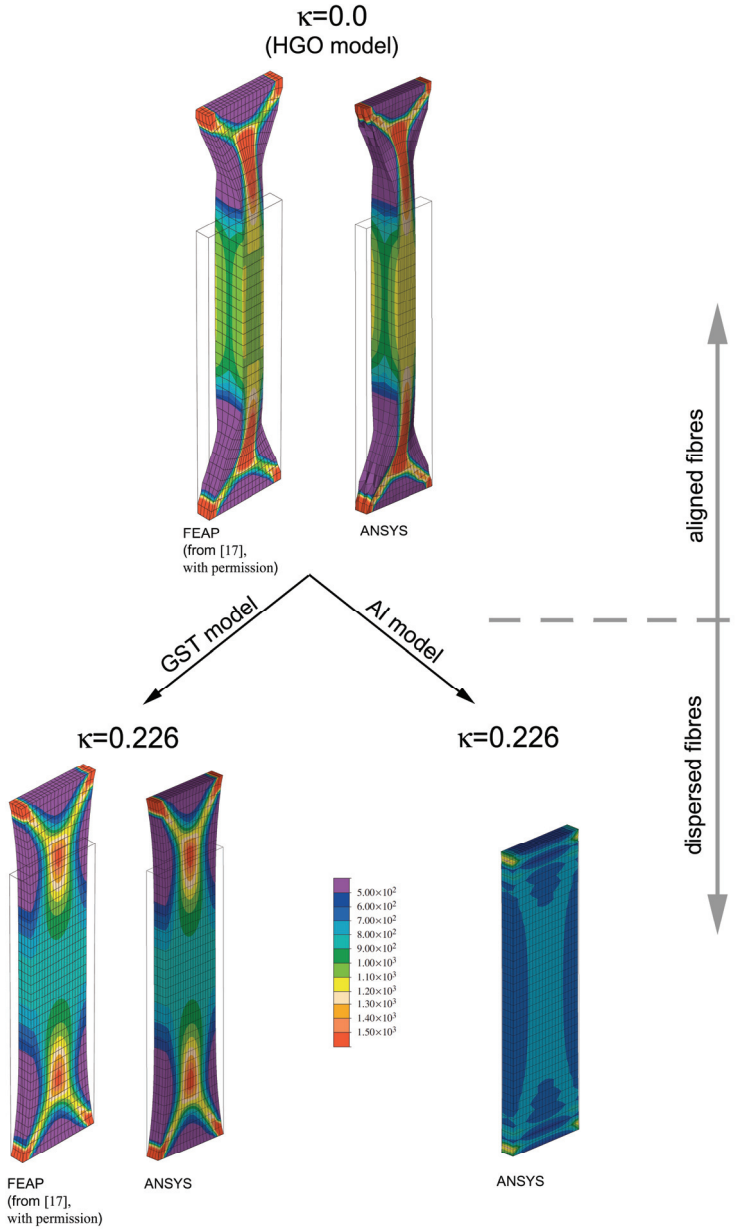

Fig. 10. Contours of Cauchy stress (kPa) in the direction of the applied load (circumferential) for different constitutive models (at $T = 1.0$ N)

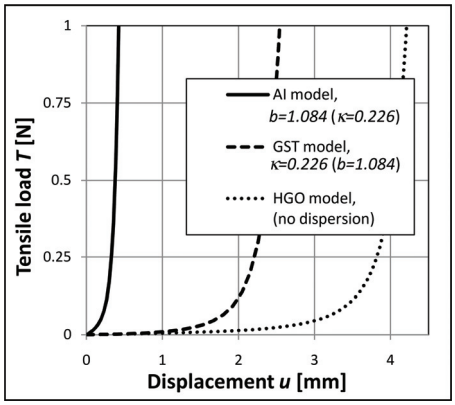

Fig. 11. Load-displacement (T–u) response for different constitutive models

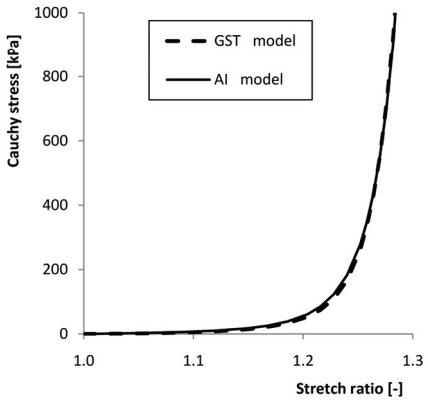

Fig. 12. Comparison of uniaxial tensile stress-stretch responses of constitutive models used for *FE* calculation

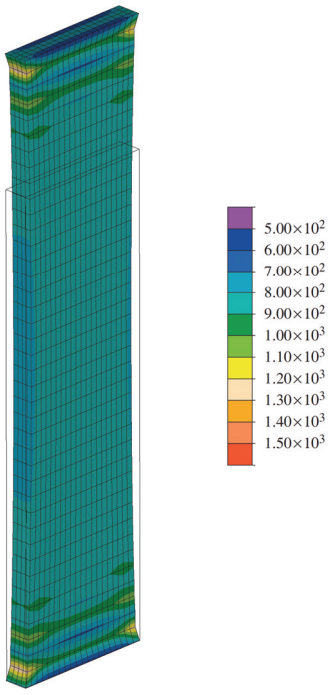

Fig. 13. Contours of Cauchy stress (kPa) in the direction of the applied load (circumferential) for AI constitutive model with modified material parameters (k_1 = 24.7 kPa, k_2 = 13.7, κ = 0.226, at T = 1.0 N)

4. Discussion

The relations between the two approaches considered to constitutive modelling (GST and AI) have been generally discussed in [31] and the specific models introduced above have been compared recently in [26]. That study concludes that there is an enormous difference between GST and AI model predictions, and there are no other publications (known to the authors of this paper) proving these results directly for the specific constitutive models. Moreover, their results related to the transversely isotropic PDF were presented only for simple tension and equi-biaxial tension conditions (both with a single fibre family) and results for two fibre families with this PDF are totally absent. In addition, their results were obtained for fixed material parameters (k_1 = 5 MPa, k_2 = 30) and limited strain range (20%). The analysis in this paper provides results for conditions more typical of arterial layers (two fibre families under a specific deformation mode with maximum stretch up to λ = 1.5). Moreover, the effects of the (progressivity) material parameter (k_2) and the effect of neglecting the fibre dispersion can both be viewed in this paper. This analysis provides also an example of finite element simulation of a realistic testing procedure that proves the applicability of the AI models and provides a comparison of GST and AI models on the basis of a non-homogenous stress field.

Despite the differences outlined above, both studies reached consistent conclusions. Study [26] specified the restriction on the dispersion parameter κ associated with the acceptable stress difference (10%) at the stretch level of λ = 1.2 and concluded it to be approx. $\kappa < 0.03 = \kappa_{max}$. The results of this paper show similar values of κ_{max} at that stretch level and even lower values of κ_{max} at higher stretches typical of vascular tissues "in vivo" (e.g., $\kappa_{max} \sim 0.01$ for λ = 1.5, k_2 = 10, φ = 45°, see Fig. 7). The results presented demonstrate that even a very low value of dispersion parameter κ (ranging roughly between 0.01 to 0.03) leads to significant (>10%) stress differences that rise progressively for higher values of κ. Such a low dispersion, however, needs not be taken into consideration (dispersion can be neglected and the GST model can then be approximated via HGO model). These results are a natural consequence of progressively non-linear (exponential) fibre stress-strain response and are also consistent with the theoretical considerations [31]. Therefore the GST model analyzed should not be understood as (computationally efficient) approximation of AI model.

Both models are clearly based on different fundamentals. AI models are based on the assumption of independent contributions of individual fibres to the total strain energy function. In the case of strongly progressive mechanical response (typical of soft tissues) this approach leads to inhomogenous distribution of tension among the differently oriented collagen fibres. No re-modelling of fibres is considered and the model is considered as perfectly elastic, which may lead to unrealistically high stress carried by individual collagen fibres (this may be viewed as a limitation of AI model). On the other hand, GST model is based on an average stretch of all fibres that may (in some cases) be viewed more credible from biomechanical point of view, especially if remodelling of collagen fibres (adjusting their reference length) is taken into account.

Generally, it is very difficult to prove which model is more credible for description of the effect of fibre angular dispersion. As shown in Fig. 12, both models are capable to follow the same single stress–strain curve even if the dispersion parameter b is known (e.g., determined histologically). In this case, however, the other structural parameters (k_1, k_2) have to reach quite different values to fit the same experimental data, although these parameters represent the same stiffness of the reinforcing fibres in principle.

A respectable approach to verification of the constitutive models would require a credible prediction of the overall stiffness of (collagen) fibres in the tissue (i.e., the amount of fibres, their cross-section area and material properties) based on microstructural analyses and on tests performed with the fibrous constituents. These data are, however, not currently available with an adequate credibility.

Direct observation of the effect of fibre angular dispersion on the resulting mechanical response is also hardly feasible because such an experimental validation would require material samples with different fibre arrangements but without varying other mechanical properties of fibres (as already discussed in [28]). These conditions are hardly realizable in the case of biological tissue.

Although the model validation is not a straightforward problem in these kinds of material, the model(s) may be validated through its overall descriptive and predictive capability for the specific material by using the results of multiple mechanical tests (with different deformation mode, and preferably also combined with microstructural investigation). This approach (but without the histological analysis) have already been used, e.g., in [33], [34] for validation of a specific AI-class model on 3D experimental data of porcine arterial media layer.

5. Conclusion

Two constitutive models, initially proposed for soft tissue, are compared, both based on exponential model for collagen fibres [16] and both accounting for the dispersion of their orientation. Although the two models share the same (or equivalent) material parameters, the analytical and numerical comparisons presented show significant differences in their predictions of the influence of fibre dispersion on the resulting macroscopic stress-strain response.

In contrast to AI model, the dispersion parameter κ of GST model cannot be understood as a purely structural parameter representing the true dispersion of fibre orientations, and therefore the GST model should be considered more phenomenological in view of the fibre dispersion. Thus, a frequent characterization of GST model as a simple extension of HGO model by the effect of fibre angular dispersion (e.g., in [28]) suffers from oversimplification; it should be considered as a model approximating this effect with a very limited accuracy. This issue is important especially under consideration of the fact that GST model has been implemented into widely used commercial FE packages (e.g., material option labelled as "*Holzapfel–Gasser–Ogden*" in ABAQUS).

The only disadvantage of the AI model is its reduced computational efficiency resulting from the necessity of numerical integration. The AI model is, for instance, capable of credibly describing the compressive behaviour of fibres based on the exact stretch of each fibre respecting its individual orientation (in contrast to GST model that controls the behaviour of the whole fibre family on the basis of the stretch in its mean orientation only). AI model is applicable for a general PDF of fibre orientation (in contrast to GST model that is limited in this aspect). AI model can also be expanded easily by any additional mechanical features of individually oriented fibres (e.g., waviness, viscoelasticity).

A significant limitation for applicability of both models compared with distributed fibre orientations is the lack of quantitative three-dimensional histological data related to distribution of (collagen) fibre orientations in biological materials. Although some data have already been published in literature, they still seem to be rather limited with respect to the complexity of the problem (distribution seems to depend strongly on the specific type of the vessel, on the specific location in the vessel and also on the specific layer of the vessel wall). As was used in many studies (e.g., [17], [20], [21], [32], [33]), the structural input data (collagen fibre distributions) can be estimated based on macroscopic mechanical data (stress-strain response) of the tissue instead of histological analyses. This approach is, however, relatively ill-conditioned and requires sufficient mechanical data. It would be beneficial to pay more attention to this issue in experimental investigation to eliminate the lack of input data and, consecutively, to support the application of AI-type constitutive models in the arteries.

Acknowledgements

This work was supported by the Czech Science Foundation, research projects No. 106/09/1732 and 13-16304S.

References

[1] VERONDA D.R., WESTMANN R.A., *Mechanical characterization of skin – finite deformations*, Journal of Biomechanics, 1970, 3, 111–124.

[2] DEMIRAY H., *A note on the elasticity of soft biological tissues*, Journal of Biomechanics, 1972, 5, 309–311, DOI: 10.1016/0021-9290(72)900047-4.

[3] DELFINO A., STERGIOPULOS N., MOORE J.E., MEISTER J.J., *Residual strain effects on the stress field in a thick wall finite element model of the human carotid bifurcation*, J. Biomech., 1997, 30, 777–786, DOI: 10.1016/S0021-9290(97)00025-0.

[4] CHUONG C.J., FUNG Y.C., *Three-dimensional stress distribution in arteries*, J. Biomech. Eng., 1983, 105, 268–274.

[5] SUN W., SACKS M., *Finite element implementation of a generalized Fung-elastic constitutive model for planar soft tissues*, Biomechanics and Modeling in Mechanobiology, 2005, 4, 190–199, DOI: 10.1007/s10237-005-0075-x.

[6] CHOI H.S., VITO R.P., *Two-dimensional stress–strain relationship for canine pericardium*, Journal of Biomechanical Engineering, 1990, 112(2), 153–159.

[7] SACKS M.S., CHUONG C.J., *Orthotropic mechanical properties of chemically treated bovine pericardium*, Annals of Biomedical Engineering, 1998, 26(5), 892–902.

[8] VANDE GEEST J.P., SACKS M.S., VORP D.A., *The effects of aneurysm on the biaxial mechanical behavior of human abdominal aorta*, Journal of Biomechanics, 2006, 39, 1324–1334, DOI: 10.1016/j.jbiomech.2005.03.003.

[9] Humphrey J.D., Yin F.C., *A new constitutive formulation for characterizing the mechanical behavior of soft tissues*, Biophysical Journal, 1987, 52(4), 563–570.

[10] CANHAM P.B., FINLAY H.M., DIXON J.G., BOUGHNER D.R., CHEN A., *Measurements from light and polarised light microscopy of human coronary arteries fixed at distending pressure*, Cardiovasc. Res., 1989, 23, 973–982.

[11] SMITH J.F.H., CANHAM P.B., STARKEY J., *Orientation of collagen in the tunica adventitia of the human cerebral artery measured with polarized light and the universal stage*, Journal of Ultrastructure Research, 1981, 77(2), 133–145.

[12] FINLAY H.M., MCCULLOUGH L., CANHAM P.B., *Threedimensional collagen organization of human brain arteries at different transmural pressures*, J. Vasc. Res., 1995, 32, 301–312.

[13] SACKS M.S., *Incorporation of experimentally-derived fiber orientation into a structural constitutive model for planar collagenous tissues*, J. Biomech. Eng., 2003, 125, 280–287, DOI: 10.1115/1.1544508.

[14] SCHRIEFL A.J., ZEINDLINGER G., PIERCE D.M., REGITNIG P., HOLZAPFEL G.A., *Determination of the layer-specific distributed collagen fibre orientations in human thoracic and abdominal aortas and common iliac arteries*, J. R. Soc. Interface, 2011, DOI: 10.1098/rsif.2011.0727.

[15] GASSER T.C., GALLINETTI S., XING X., FORSELL C., SWEDENBORG J., ROY J., *Spatial orientation of collagen fibers in the abdominal aortic aneurysm's wall and its relation to wall mechanics*, Acta Biomater., 2012, 8, 3091–3103.

[16] HOLZAPFEL G.A., GASSER T.C., OGDEN R.W., *A new constitutive framework for arterial wall mechanics and a comparative study of material models*, Journal of Elasticity, 2000, 61, 1–48, DOI: 10.1023/A:1010835316564.

[17] GASSER T.C., OGDEN R.W., HOLZAPFEL G.A., *Hyperelastic modelling of arterial layers with distributed collagen fibre orientations*, J. R. Soc. Interface, 2006, 3, 15–35, DOI: 10.1098/rsif.2005.0073.

[18] WUYTS F.L., VANHUYSE V.J., LANGEWOUTERS G.J., DECRAEMER W.F., RAMAN E.R., BUYLE S., *Elastic properties of human aortas in relation to age and atherosclerosis: a structural model*, Phys. Med. Biol., 1995, 40, 1577–1597, DOI: 10.1088/0031-9155/40/10/002.

[19] HURSCHLER C., LOITZ-RAMAGE B., VANDERBY Jr. R., *A structurally based stress-stretch relationship for tendon and ligament*, J. Biomech. Eng., 1997, 119, 392–399.

[20] ZULLIGER M.A., FRIDEZ P., HAYASHI K., STERGIOPULOS N., *A strain energy function for arteries accounting for wall composition and structure*, J. Biomech., 2004, 37, 989–1000, DOI: 10.1016/j.jbiomech.2003.11.026.

[21] BILLIAR K.L., SACKS M.S., *Biaxial mechanical properties of the native and glutaraldehyde-treated aortic valve cusp:* Part II *– A structural constitutive model*, J. Biomech. Eng., 2000, 122, 327–335, DOI: 10.1115/1.1287158.

[22] LANIR Y., *Constitutive equations for fibrous connective tissues*, J. Biomech., 1983, 16, 1–12, DOI: 10.1016/0021-9290(83)90041-6.

[23] ELSHEIKH A., KASSEM W., JONES S.W., *Strain-rate sensitivity of porcine and ovine corneas*, Acta Bioeng. Biomech., 2011, 13(2), 25–36.

[24] PANDOLFI A., HOLZAPFEL G.A., *Three-dimensional modeling and computational analysis of the human cornea considering distributed collagen fiber orientation*, J. Biomech. Eng., 2008, 130, 061006.

[25] ANNAIDH A., BRUYERE K., DESTRADE M., GILCHRIST M.D., MAURINI C., OTTENIO M., SACCOMANDI G., *Automated estimation of collagen fibre dispersion in the dermis and its contribution to the anisotropic behaviour of skin*, Ann. Biomed. Eng., 2012, 40(8), 1666–1678, DOI: 10.1007/s10439-012-0542-3.

[26] CORTES D.H., LAKE S.P., KADLOWEC J.A., SOSLOWSKY L.J., ELLIOT D.M., *Characterizing the mechanical contribution of fiber angular distribution in connective tissue: comparison of two modelling approaches*, Biomech. Model. Mechanobiol., 2010, 9, 651–658, DOI: 10.1007/s10237-010-0194-x.

[27] LOKSHIN O., LANIR Y., *Micro and macro rheology of planar tissues*, Biomaterials, 1983, 30, 3118–3127, DOI: 10.1016/j.biomaterials.2009.02.039.

[28] HOLZAPFEL G.A., *Collagen in arterial walls: Biomechanical aspects*, [in:] Fratzl P (ed.) Collagen, 2008, Springer Science +Business Media, 285–324.

[29] LEBEDEV V.I., *Quadratures on a sphere*, Zh. Vychisl. Mat. Mat. Fiz., 1976, 16(2), 293–306, DOI: 10.1016/0041-5553(76)90100-2.

[30] SKACEL P., BURSA J., *Numerical implementation of constitutive model for arterial layers with distributed collagen fibre orientations*, Computer Methods in Biomechanics and Biomedical Engineering, 2013, DOI: 10.1080/10255842.2013.847928.

[31] FEDERICO S., HERZOG W., *Towards an analytical model of soft biological tissues*, J. Biomech., 2008, 41, 3309–3313, DOI: 10.1016/j.jbiomech.2008.05.039.

[32] SKACEL P., BURSA J., *Material parameter identification of arterial wall layers from homogenized stress-strain data*, Computer Methods in Biomechanics and Biomedical Engineering, 2010, 14(01), 33–41, DOI: 10.1080/10255842.2010.493516.

[33] HOLLANDER Y., DURBAN D., LU X., KASSAB G.S., LANIR Y., *Experimentally validated microstructural 3D constitutive model of coronary arterial media*, J. Biomech. Eng., 2011, 133, 031007-1–031007-14.

[34] HOLLANDER Y., DURBAN D., LU X., KASSAB G.S., LANIR Y., *Constitutive modeling of coronary arterial media - comparison of three model classes*, J. Biomech. Eng., 2011, 133, 061008-1–061008-12.